Available online at www.sciencedirect.com
SCIENCE DIRECT®
Journal of Chromatography A, 1086 (2005) 83–90
JOURNAL OF CHROMATOGRAPHY A
www.elsevier.com/locate/chroma

Statistical methods for comparing comprehensive two-dimensional gas chromatography–time-of-flight mass spectrometry results: Metabolomic analysis of mouse tissue extracts

Robert A. Shellie [a], Werner Welthagen [b,c], Jitka Zrostliková [d], Joachim Spranger [e,f], Michael Ristow [e,f], Oliver Fiehn [a,g], Ralf Zimmermann [b,c,h,*]

[a] *Max Planck Institute of Molecular Plant Physiology, Potsdam-Golm, Germany*
[b] *Institute of Ecological Chemistry, GSF-Research Centre, Oberschleissheim, Germany*
[c] *Analytical Chemistry, University of Augsburg, Augsburg, Germany*
[d] *Leco Instruments, Prague, Czech Republic*
[e] *German Institute of Human Nutrition, Potsdam-Rehbrücke, Germany*
[f] *Charité University of Medicine, Berlin, Germany*
[g] *UC Davis Genome Center, University of California Davis, Davis, CA, USA*
[h] *BIfA, Bavarian Institute of Applied Environmental Research and Technology, Augsburg, Germany*

Available online 27 June 2005

Abstract

The potential for the utilization of GC × GC–time-of-flight (TOF) MS for high-resolution metabolomics studies is discussed, with the implementation of some statistical comparisons for biomarker detection. Metabolite profiles from NZO obese mice versus BL/6 control mice are compared and contrasted using a number of chromatogram comparison routines, including direct chromatogram comparisons, chromatogram subtraction and averaging routines, as well as a method for generating relative weighted peak surface difference chromatograms, and a more conventional Student's *t*-test statistical approach.

Keywords: Gas chromatography, comprehensive two-dimensional; Mass spectrometry, time-of-flight; Metabolomics; Data processing

1. Introduction

With an unsurpassed capability for generating overall peak resolution, and with important attributes like ordered, readily interpretable chromatograms [1], as well as enhanced sensitivity [2], GC × GC offers great advantages over conventional (1D) GC. These advantages have proven to be useful in various fields—which include, but are not limited to forensic analysis [3], flavor and fragrance quality control [4,5], process monitoring [6], environmental aerosol analysis [7] and metabolomics [8,9]. The abovementioned applications are similar in that they all essentially strive to find markers that indicate the normality/abnormality of the sample. In each of these applications there will be a potential requirement to analyze a high number of samples, after which reliable approaches to compare the results is necessary. The present investigation is concerned with the comparison of GC × GC–TOF-MS chromatograms for high throughput metabolomics purposes.

Metabolite levels can be regarded as the ultimate response of biological systems to genetic or environmental changes since they are the end products of cellular regulatory processes. LC–MS and GC–MS metabolomic strategies have found their place in the field of plant biology over the last few years [10]. Similarly, strategies for metabolite flux analysis in bacteria have been described using GC–MS [11], as well as the use of global fingerprinting strategies for mammalian biology using NMR [12]. While rapid at-clinic techniques for predicting the risk of metabolic disease in humans may

* Corresponding author. Tel.: +49 89 3187 4544; fax: +49 89 3187 3371.
E-mail address: ralf.zimmermann@gsf.de (R. Zimmermann).

0021-9673/$ – see front matter © 2005 Elsevier B.V. All rights reserved.
doi:10.1016/j.chroma.2005.05.088

be seen as the Holy Grail of metabolomics, one of the interim goals is to characterize a diversity of biological systems in terms of their global metabolite profiles—or their so called metabolome. It is hoped that such screening studies will result in biomarker discovery, or at the very least this should provide discriminatory power that relates the metabolome to a unique phenotype.

Previously, we have illustrated the suitability of GC × GC–TOF-MS for metabolomics by reporting the analysis of derivatized mouse tissue extracts [8]. The increased number of peaks in GC × GC–TOF-MS chromatograms compared to GC–TOF-MS chromatograms was highlighted. The overall enhancement of spectral purity in GC × GC–TOF-MS, which improves mass spectral deconvolution and similarity matches, is a most important feature. GC × GC–TOF-MS is directly applicable to differential metabolomic analysis, but owing to the expected large biological variability there is a requirement to perform a sufficient number of biological replicates in order to ensure that statistically significant findings are presented. Fiehn showed that quantitative differences, in metabolite levels in plants caused by extraction, chemical modification (derivatization) and analysis by GC–MS, are small when compared to the biological variability within samples [13]. Indeed biological variation (in plants) generally exceeds instrumental error by an order of magnitude [14]. Thus, a general rule of thumb for metabolomics demands that 10 or more replicate analyses are performed for each diverse system.

In addition to a general need to minimize the analysis time, such high throughput GC × GC–TOF-MS studies should be supported by an approach for comparing the resulting chromatograms. The use of automated statistical procedures is of utmost importance in high sample throughput GC × GC studies and up to now research has been lagging in this regard. In this investigation we propose some different statistical methods for the evaluation of the differences in GC × GC chromatograms.

2. Experimental

2.1. Instrumentation

GC × GC–TOF-MS analysis was performed using an Agilent 6890N gas chromatograph (Agilent Technologies, Palo Alto, CA, USA) fitted with a Leco GC × GC system (Leco, St Joseph, MI, USA) that consisted of a dual stage, four-jet (two warm and two cold) cryogenic modulator and second dimension GC oven. The GC system was coupled to a Pegasus III time-of-flight mass spectrometer (Leco Corporation). Separate instruments were used to perform the two methods described below. Operating conditions are given in Table 1.

2.2. Samples

Mice were housed in standard barrier facilities, according to the Federation of European Laboratory Animal Science Associations (FELASA) regulations, and were fed standard chow (Altromin, Lage, Germany). Tissues were collected from five individual 10 months old non-fasted female, lean C57BL/6 control strain mice, and five separate 10 months old fasted female lean C57BL/6 mice. Tissues were also collected from five separate 10 months old non-fasted female obese NZO strain mice, as well as from four individual 10 months old male non-fasted NZO strain mice. five milligrams fresh weight samples were extracted at −15 °C with 1 mL of a mixture of degassed H_2O:MeOH:$CHCl_3$ (2:5:2, v/v/v) and shaken for 5 min at 4 °C according to the procedure described by Weckwerth et al. [15]. A 500 μL aliquot was concentrated to complete dryness.

2.3. Derivatization

Methyl oxime derivatives were produced by dissolving the dry extracts in 20 μL of freshly prepared *O*-methylhydroxylamine·HCl (40 mg/mL in pyridine) and

Table 1
Details of GC × GC and MS method parameters for Method A and Method B

	Method A	Method B
GC × GC parameters		
First dimension column	Polydimethyl siloxane 30 m; 250 μm I.D.; 0.25 μm d_f	5% phenyl polydimethyl siloxane 30 m; 250 μm I.D.; 0.25 μm d_f
Second dimension column	50% phenlyl polysilphenylene siloxane 1.5 m; 100 μm I.D.; 0.10 μm d_f	50% phenlyl polysilphenylene siloxane 2.0 m; 100 μm I.D.; 0.10 μm d_f
Main oven T program	50 °C (8 min) 5 °C/min to 310 °C	85 °C (2 min) 7 °C/min to 270 °C 20 °C/min to 330 °C 330 °C (5 min)
Second oven T program	56 °C (10 min) to 300 °C at 5 °C/min	+10 °C with respect to ^{1}D oven
Modulation period	3.0 s	2.5 s
Carrier gas (He) flow rate	1 mL/min	1 mL/min
Injected volume/split ratio	1.0 μL/1:2[a]	0.2 μL/splitless (90 s)
MS parameters		
Transfer line T	280 °C	300 °C
Ion source T	250 °C	250 °C
Detector voltage	−1800 V	−1900 V
Data rate	100 spectra/s, 40–400 *m/z*	200 spectra/s, 85–500 *m/z*

[a] A split ration of 1:2 was chosen due to technical difficulties to run the Atas Optic 3 injector under splitless conditions.

incubated at 30 °C for 90 min with continuous shaking. Subsequent trimethyl silylation was achieved by the addition of 80 μL of *N*-methyl-*N*-trimethylsilyltrifluoroacetamide, followed by continuous shaking for 30 min at 37 °C.

2.4. Software

Leco ChromaTOF software was used throughout to control the instruments, as well as to acquire and process (including automated peak deconvolution of) the data. A Leco ChromaTOF software feature was utilized to perform automated chromatogram comparisons as part of the present study. Retention time information (^1t_R and ^2t_R) as well as the full mass spectrum of selected peaks were automatically stored as reference data. The peak response variation tolerance was kept at the default value of 20% because differences in peak responses were expected. A mass spectrum similarity threshold of 500/1000 was used appropriate for this purpose. This was sufficiently low to minimize false negatives but must also be high enough to ensure that the number of false positives is limited. In determining the retention time window parameters for peak-comparison, ^1t_R variations of more than one modulation period (P_M), were disallowed. Second dimension retention time variations of 0.1 s were set, since this was of the order of the typical peak widths of non-tailing peaks.

3. Results and discussion

3.1. Method development for metabolomics

While a general recommendation for GC × GC states that a minimum of three to four second dimension peak slices should be taken from each peak that elutes from the first dimension column [16–18], in some cases, such a constraint is counterproductive. Separations that are not textbook comprehensive can also produce satisfactory results. With sufficient second dimension resolution as well as mass spectrometric resolution, then having fewer slices causes nothing to be lost. This will often provide a direct route to reducing the analysis time, which is desirable for studies that require the analysis of great numbers of samples. Since data file sizes are proportional to analysis time, this realizes a second benefit, in terms of data handling and storage (archiving). Thus, *Method A* was designed to satisfy the modulation rule, but this was ignored in *Method B*. Some differences with respect to separation (chromatograms not shown) were observed between the two methods used in this investigation, ultimately however they have little or no impact on the final results.

The MS parameters used in the present study were based upon our validated GC–TOF-MS method [21] for metabolomics, which uses a mass range of 415 u (85–500 *m*/*z*). Fast data acquisition rates were used, both to ensure accurate quantitative measurement of the narrow peaks generated by the modulation process, and to maximize the effectiveness of mass spectral deconvolution. Deconvolution requires fast data acquisition (e.g. 100–200 Hz for very-fast GC). GC × GC analyses are often long, and the use of high spectra acquisition rates becomes somewhat prohibitive in terms of data file size. A single 60 min analysis where 200 spectra/s are collected over 415 *m*/*z* requires in excess of 570 Mb of disk space. In contrast, by reducing the analysis time to ∼37 min (Method B) the file size is reduced by approximately 320 Mb. Accurate peak deconvolution relies upon having sufficient data density, and having carefully examined the results from two GC × GC–TOF-MS methods (which used different spectra acquisition rates) we suspect that 100 spectra/s should also be sufficient for accurate detection in the faster (37 min) method. In this case a typical data file should not exceed 125 Mb.

GC × GC–TOF-MS chromatograms (not shown) of each tissue extract of non-fasted female BL/6 mice were acquired using either Method A or Method B. Note, that since the two methods were developed independently in separate laboratories there has not been a direct comparison of the chemical profile of the different tissue extracts, nonetheless, the different tissues could be clearly set apart. The diversity of the tissues indicated that some may ultimately be better suited than others for highlighting phenotypic differences.

3.2. Comparison of chromatograms

Chemometric analysis of comprehensive two-dimensional separations (ref. [22], and references therein) has the potential to extend the information gained from GC × GC separations. However, there is still work required for such approaches to be fully utilized, especially in the development of algorithms for retention time alignment of two-dimensional chromatographic data. In comparing different metabolic profiles with one another we have proposed a number of possible strategies.

3.2.1. Direct chromatogram comparison and chromatogram averaging

Fig. 1 shows in the left column four BL/6 female spleen samples and in the column on the right four NZO female spleen samples. These samples can be directly compared to one another by eye. If the samples are analyzed in a reproducible fashion the chromatograms can be added up or averaged, as shown in the two larger chromatograms in the middle of Fig. 1. A summation of the TIC chromatograms was performed in this case. However, it is difficult to detect differences in the full chromatograms. Thus, a small section (indicated with two boxes in the middle figures of Fig. 1) was extracted and used for the evaluation of the samples (Fig. 2)

Some differences can be seen in the extracted sections even by means of visual inspection (Fig. 2). These differences are primarily based on concentration differences in the two samples, which result in a change in color intensities of the two samples compared. Some of the areas where differences can be spotted are encircled. Compounds corresponding with the *t*-test evaluation (described later) are indicated by arrows and

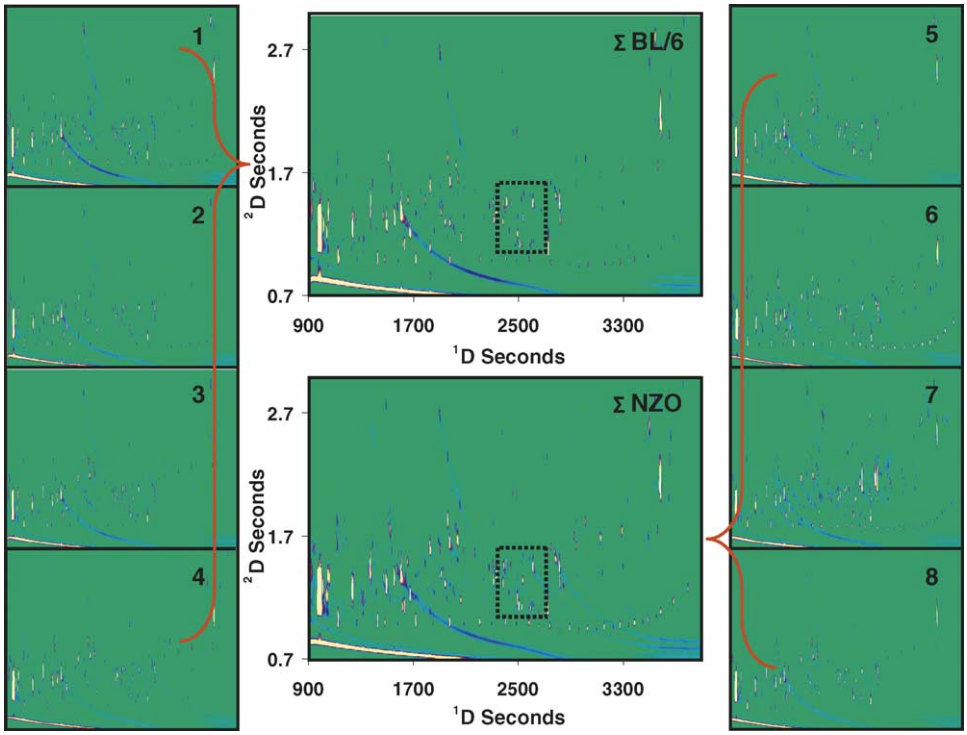

Fig. 1. Comparison of GC × GC–TOF-MS (TIC) chromatograms of spleen tissue from NZO obese mice (right column, 5–8) with BL/6 control mice (left column, 1–4). The two middle GC × GC–TOF-MS (TIC) chromatograms show the results from a direct summation of the four NZO and four BL/6, respectively chromatograms. The boxes drawn in the two central summed GC × GC–TOF-MS (TIC) chromatograms indicate a region used for biomarker determination.

are marked with their assigned *t*-test numbers. It is important that the color scaling on both samples corresponds to the same relative peak heights, for future work it would be advised to use internal standards to normalize the data sets.

3.2.2. *Bubble plot representation of GC × GC–TOF-MS data*

Although the method of direct comparison could be performed quite easily, a lot of information generated by GC × GC–TOF-MS is lost. In GC × GC–TOF-MS compounds are not only separated chromatographically, but also separated by deconvolution of the mass spectra generated by TOF-MS detection. The use of the deconvoluted peaks could thus reveal many more underlying differences in the two samples. The introduction of bubble plots in the analysis of GC × GC–TOF-MS data [7] makes use of the peak tables generated by the Leco ChromaTOF software (after peak deconvolution) and presents them in a visual perspective where bubbles represent the individual peaks and bubble sizes correspond to the integrated peak areas. The peaks identified in four BL/6 mice and four NZO mice were firstly normalized and then added together to create two bubble plots (Fig. 3). This was achieved on a basis of normalizing the peaks in the extracted area to the total area of all the

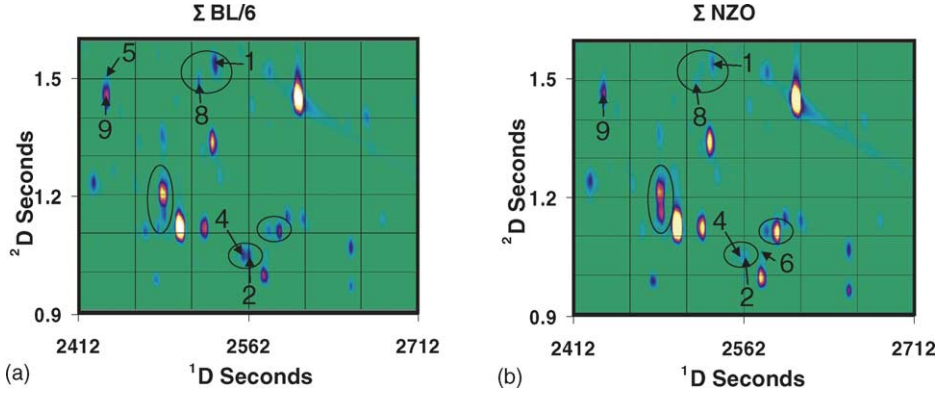

Fig. 2. Expanded sections from the summed GC × GC–TOF-MS (TIC) chromatograms (indicated in Fig. 1 with encircled areas where differences in the color intensity (i.e. peak concentration differences) occur. The peaks indicated by arrows correspond to peaks identified with the *t*-test method (see Fig. 6).

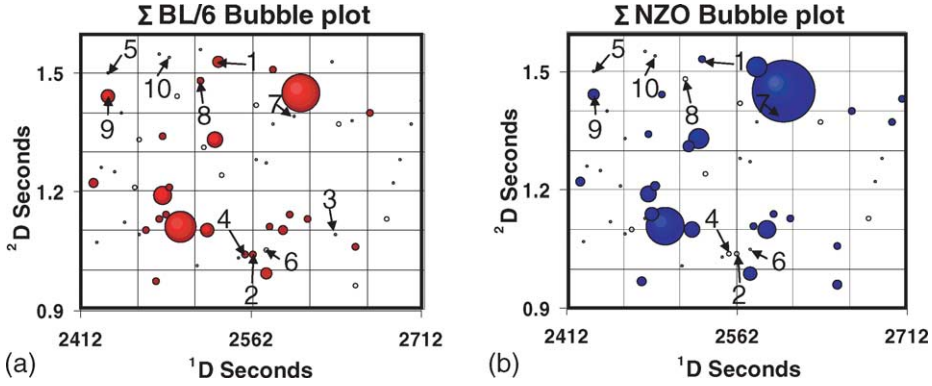

Fig. 3. Bubble plot representation of the deconvoluted peak tables generated by summation of the areas of the compounds in the two samples groups examined. Arrows are indicating peaks corresponding with *t*-test assigned values (see Fig. 6).

peaks (excluding artifact peaks). Normalization is necessary to eliminate possible changes in sample volume or any other factors that could influence the detection and quantification. Internal standards could be used instead of using the total peak area as a reference for the normalization. Arrows are used to highlight differences between the two summed bubble plots. These also correspond with the *t*-test values that are discussed later. Some of the differences corresponding to those encircled in Fig. 2 are now more obvious. This is already a big improvement, but changes occurring in compounds of low concentration cannot be seen unless the bubble sizes are scaled appropriately.

3.2.3. Difference chromatograms

The approach of directly subtracting chromatograms from one another also reveals differences in samples. We stress however that reproducible results are critical for this approach. The two summed chromatograms illustrated earlier were used to investigate this approach. When subtracting two ideally identical samples from one another only the base line (i.e. the empty 2D chromatographic surface) should remain. However, if there are any peaks concentration differences in the two subtracted samples both negative and positive peaks should result upon the subtraction procedure. Fig. 4a shows a subtracted chromatogram (BL/6–NZO). The positive peaks are visible (i.e. the compounds with higher peak intensity in the summed BL/6 chromatogram) while Fig. 4b shows the resulting negative peaks (i.e. corresponding to higher peak intensities in the NZO chromatograms). Medium to high relative peak intensity differences between the NZO and BL/6 chromatograms can easily be spotted for the major compounds in the subtracted chromatograms. Differences in minor peaks are of course more difficult to detect.

3.2.4. Normalizing peak surfaces for generation of difference chromatograms

A higher significance, however, can be obtained if the method of direct subtraction is used for the deconvoluted peak data set. In Fig. 5a, the bubble plot representation of the data set resulting from the subtraction of the NZO peak surfaces from the respective BL/6 peak surfaces is given (BL/6–NZO). Fig. 5a shows good comparison with Fig. 4a, but, it is still problematic to identify differences in low concentration compounds (i.e. small bubbles in Fig. 3). In other words, it would be desirable to see solely the relative peak surface changes but not the absolute ones. This drawback of direct subtraction can be overcome by using a peak surface normalized subtraction approach, which is shown in the following example on the

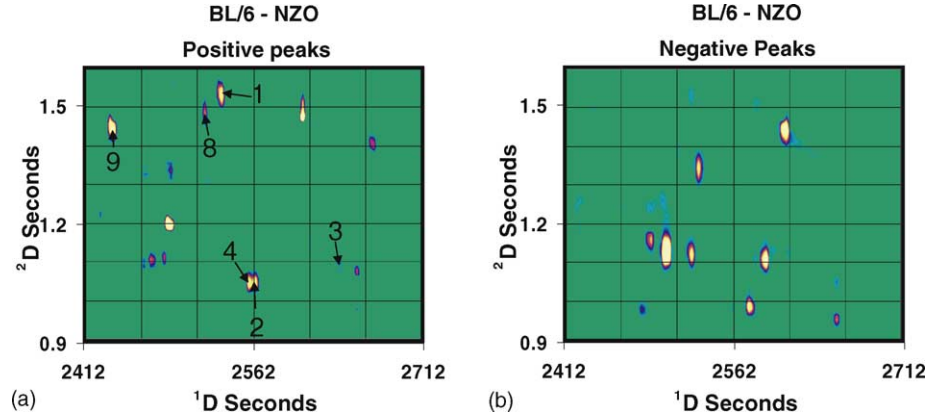

Fig. 4. Direct subtraction of the summed NZO obese mice GC × GC–TOF-MS (TIC) chromatogram from the summed BL/6 control mice GC × GC–TOF-MS (TIC) chromatogram showing the resulting positive peaks in (a) and the negative peaks in (b).

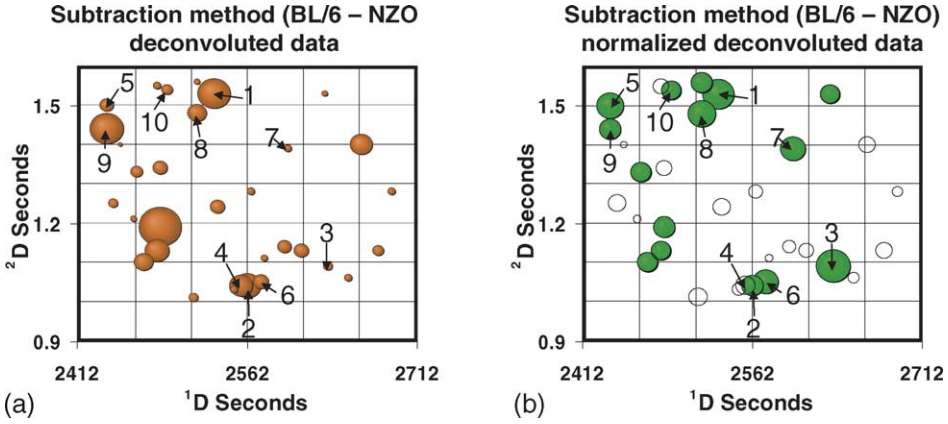

Fig. 5. (a) The direct subtraction of the normalized bubbles (peaks) of the averaged NZO sample from the bubbles of the averaged BL/6 mice sample. (b) The direct subtraction of the normalized bubbles (peaks) of the averages NZO sample from the bubbles of the averages BL/6 mice sample divided by the standard deviation factor (for details see text). The 15 highest peaks are indicated in green color, and arrows indicate the peaks corresponding with the *t*-test bubbles.

BL/6–NZO case. We are starting from the averaged BL/6 and NZO samples ($n = 4$ in both cases) with i peaks (in the section of the chromatogram under consideration i = number of peaks). Firstly, i normalization factors $N_{i\,\mathrm{BL/6}}$ are calculated which transform the peak surface $S_{i\,\mathrm{BL/6}}$ of the ith peak in the BL/6 sample to the unity value c according to the formula

$$S_{i\,\mathrm{BL/6}} N_{i\,\mathrm{BL/6}} = c$$

with $N_{i\,\mathrm{BL/6}} = c(S_{i\,\mathrm{BL/6}})^{-1}$ and c being a constant (i.e. $c = 1$). Subsequently the normalization factors $N_{i\,\mathrm{BL/6}}$ are applied on the respective ith peak surface values $S_{i\,\mathrm{NZO}}$ of the NZO sample:

$$S_{i\,\mathrm{NZO}} N_{i\,\mathrm{BL/6}} = S_{i\,\mathrm{NZOnorm}}$$

By subtraction of the obtained $S_{i\,\mathrm{NZO\_norm}}$ from c one get the relative peak surface difference $S_{i\,\mathrm{BL/6–NZOrel}}$ of the ith peak:

$$S_{i\,\mathrm{BL/6-NZOrel}} = c - S_{i\,\mathrm{NZO\_norm}}$$

A common phenomenon in biological samples, however, is bio-diversity. The concentration of the same compound in a target tissue can differ from specimen to specimen and even from day to day within the same specimen. By the abovementioned peak surface normalized subtraction approach, the relative differences between small peaks have the same impact as the relative differences between larger peaks. However, as the number n of the respective averaged chromatographic NZO and BL/6 samples is rather low) it is appropriate to consider the standard deviation σ_i of the ith peak surface with $\sigma_i = (\sigma_{i\,\mathrm{NZO}} + \sigma_{i\,\mathrm{BL/6}})/2$ By dividing the relative peak surface difference $S_{i\,\mathrm{BL/6–NZOrel}}$ by the standard deviation σ_i the relative weighted peak surface difference $S_{i\,\mathrm{BL/6–NZOwigrel}}$ are obtained which are a good measure for significant peak surface differences between the two averaged samples:

$$S_{i\,\mathrm{BL/6-NZOwigrel}} = \frac{S_{i\,\mathrm{BL/6-NZOrel}}}{\sigma_i}$$

In Fig. 5b, the resulting relative weighted peak surface difference ($S_{i\,\mathrm{BL/6–NZOwigrel}}$) values are depicted in a bubble plot representation (i.e. the division by the standard deviation factors σ_i reduces the bubble size of compounds prone to bigger deviations). The output bubble sizes indicate the metabolites in the control BL/6 mice samples that are of higher concentration compared to the NZO mice, weighted according to the intra-sample variability. The comparison of Fig. 5a and b depicts that the normalization method puts emphasis on some compounds which only exhibit a minor absolute peak size difference (i.e. small sizes in Fig. 5a). The 15 highest $S_{i\,\mathrm{BL/6–NZOwigrel}}$ values are considered as potential biomarker candidates and are indicated in Fig. 5b by filled printing (green color).

3.2.5. *t*-Test comparison

In the work reported earlier [8], we showed some *t*-test values for a few selected metabolites in the same extracted region. These metabolites were selected by visual comparison of the different chromatograms. For a full evaluation of the proposed use of Student's *t*-test in finding potential biomarkers all the peaks identified and deconvoluted in the extracted chromatographic area were subjected to the same *t*-test comparison. Fig. 6 shows the bubble plot of the inverse of the *t*-test value. Thus, a larger bubble corresponds to a larger probability of being a biomarker. The peaks are numbered according to their bubble size, with 1 being the largest. Table 2 shows these indicated bubbles along with the corresponding results from the normalized bubble subtraction method.

The results obtained in all of these proposed comparison methods pointed to the same potential biomarkers discussed in ref. [8] and it also showed some other compounds previously overlooked due to low compound concentrations. Based on the final *t*-test results the 10 highest peaks are compared in each of the above methods. From the direct comparison of the summed chromatograms only 4 of the 10 peaks correspond, while 6 of the 10 *t*-test peaks correspond

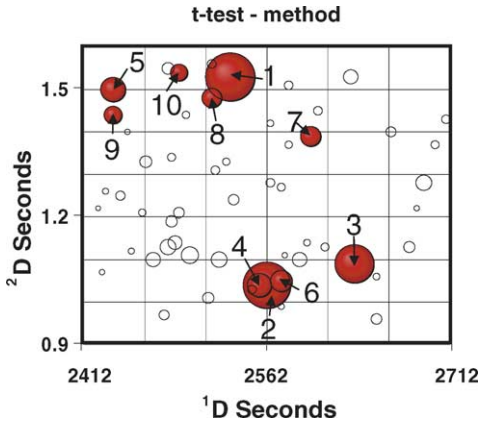

Fig. 6. Bubble plot of the inverse of the *t*-test values obtained by comparing the BL/6 control mice with the NZO obese peak tables. The 10 peaks that show the highest degree of difference are indicated in red and assigned numbers according to their respective bubble size.

in the bubble plot of the summed peak tables. The subtraction method using the summed chromatograms also shows six corresponding peaks. All three of these methods however also show other peaks that exhibit changes in concentration, but due to the variability of these peaks in the same sample set they do not show up in the *t*-test plot.

The bubble plot subtraction method, with the correction factor for variations, contains 9 out of the 10 peaks highlighted as being significant by *t*-tests. Furthermore, the 20 largest bubbles using this approach correspond to 17 of the most significant components (as determined by *t*-test). This indicates that these two approaches are essentially equivalent (in terms of efficacy) for use in biomarker identification. These bubble plot interpretations are, however, not done automatically yet and require considerable effort to arrange the peak tables in spreadsheets to obtain a suitable (and consistent) order. Recently we applied successfully a Fisher-value approach for detection of the metabolites relevant for discrimination between NZO and BL/6 mice, with results similar to the ones obtained by the *t*-test method. The top Fisher-values subsequently were used as input-variables for a principal component analysis (PCA). In the PCA plot the quality of the class separation (NZO, BL/6) can be easily visualized [23].

3.2.6. Automated peak comparison

The inconsistencies in the peak tables make it difficult to place the peak information into a suitable matrix format, where rows represent an individual peak, columns represent individual chromatograms, and the values are peak intensities. The comparison feature in the Leco ChromaTOF software simplifies the task of sorting the peak tables, since all chromatograms, having been compared to a reference contain the same number of peaks. All exported peak tables are also in a consistent order, and the peak intensities (areas) can be cut-and-pasted directly into a spreadsheet.

Table 2
The *t*-test values of the compounds that show the highest probability of being biomarkers and their corresponding relatively weighted peak surface obtained from the normalized subtraction method

Rank number of *t*-test (Fig. 6)	t-test value	Compound name (NIST)	Relative weighted peak surface difference values (rank) (Fig. 5b)
1	0.0068	4-Ketoglucose, methoxy, silyl	231.8 (2)
2	0.0072	Sugar alcohol	109.5 (8)
3	0.0106	Unknown	267.0 (1)
4	0.0257	Unknown	173.9 (4)
5	0.0265	Sugar alcohol	91.6 (16)
6	0.0329	Unknown	146.6 (6)
7	0.0381	Sugar alcohol	153.1 (5)
8	0.0392	Unknown	107.9 (3)
9	0.0490	Unknown	113.3 (4)
10	0.0515	Unknown	95.5 (14)

Table 3
List of the metabolites exhibiting the most significant differences in relative abundance in NZO and BL/6 mice

Name (tent)	^1t_R (s)	^2t_R (s)	*t*-test	*X*-fold obese	*X*-fold lean
Oxamic acid	725	1.8	0.002	+4.1×	
Unknown aromatic amine	793	1.8	0.006	+1.5×	
Succinic acid	915	2.0	0.008	+1.8×	
Aliphatic compound	950	1.8	0.003		+4.8×
Trihydroxybutyric acid	1163	1.8	0.006		+1.3×
Creatinine enol	1175	2.0	0.005	+6.4×	
Ornithine	1410	1.9	0.004	+4.0×	
Hypoxanthine	1415	2.4	0.001	+15.1×	
Myristic acid	1445	2.0	0.001	+5.2×	
D-Glucose	1578	1.8	0.008	+2.2×	
Octadecenoic acid	1730	2.1	0.001	+4.7×	

The values in the *X*-fold columns indicate the relative differences in the abundance of these metabolites between the two classes.

The compare function was used to automatically compile a peak list for a set of nine kidney samples as an example. Student's *t*-tests were performed to determine differences in the two sets of samples. A brief list of the metabolites that exhibit the most significant differences between obese and lean mice is given in Table 3. Tentative identification is given for some of these major components. Metabolite identification was achieved by comparing the experimentally derived mass spectra with a library database of metabolite mass spectra, as well as with commercial MS libraries. Currently our metabolite library contains around 500 spectra that have been recorded by analysing authentic standards. Whilst the purity of the GC × GC–TOF-MS spectra is generally high, leading to good quality library matches, many peaks remain unassigned because they are not present in any of these libraries. In this preliminary study we have not incorporated our standard retention time markers, which will be added, as the method for high throughput metabolomics is refined.

4. Conclusion

GC × GC–TOF-MS is now a readily available tool for high-resolution metabolomics.

Tissue extracts from obese NZO mice and lean BL/6 mice were compared using direct chromatogram comparisons, and by employing chromatogram subtraction and averaging routines. An additional method for generating relative weighted peak surface difference chromatograms compared favorably with a more conventional Student's *t*-test statistical approach for determining differences in the samples, indicating that the latter two approaches are essentially equivalent (in terms of efficacy) for use in biomarker identification. The comparison routines presented here were performed on TIC chromatogram data and as a consequence they are equally transferable for use with GC × GC–FID data (although the benefit of peak deconvolution will be lost). It is important to note that the number of replicates performed throughout these studies may be insufficient to produce statistical significant results, nonetheless, as a proof-of-concept it can be shown that GC × GC–TOF-MS is useful for differentiating NZO and BL/6 mice based upon their individual metabolomes.

Acknowledgements

This work was funded through the Max-Planck-Society and the German Ministry of Education and Research (BMBF), GSF-Research Center, BioProfile Nutrigenomics Berlin/Brandenberg, BMBF project number 0313036B/C. The authors gratefully acknowledge the help of Peter Tablack (Leco Germany). We thank Änne Eckardt for quality control of extraction and GC–TOF-MS standard operating procedures. Werner Welthagen thanks the Bayerische Forschungsstiftung (BFS) for a scholarship. Michael Ristow is funded by the Deutsche Forschungsgmeinschaft and Fritz-Thyssen-Stiftung. We are grateful for the provision of NZO mice by Dr. R. Kluge and Dr. H.G. Joost, and wish to acknowledge Dr. C. Thöne-Reinecke for assisting with animal handling.

References

[1] E.B. Ledford, J.B. Phillips, J.Z. Xu, R.B. Gaines, J. Blomberg, Am. Lab. 28 (1996) 22.
[2] A.L. Lee, K.D. Bartle, A.C. Lewis, Anal. Chem. 73 (2001) 1330.
[3] G.S. Frysinger, R.B. Gaines, J. Forensic Sci. 47 (2002) 471.
[4] R. Shellie, P. Marriott, A. Chaintreau, Flavour Fragr. J. 19 (2004) 91.
[5] C. Debonneville, A. Chaintreau, J. Chromatogr. A 1027 (2004) 109.
[6] K. Sun, W. Winniford, J. Griffith, J.K. Colura, S. Green, M. Pursch, J. Luong, J. Chromatogr. Sci. 41 (2003) 506.
[7] W. Welthagen, J. Schnelle-Kreis, R. Zimmermann, J. Chromatogr. A 1019 (2003) 233.
[8] W. Welthagen, R.A. Shellie, J. Spranger, M. Ristow, R. Zimmermann, O. Fiehn, Metabolomics 1 (2005) 57.
[9] A.E. Sinha, J.L. Hope, B.J. Prazen, E.J. Nilsson, R.M. Jack, R.E. Synovec, J. Chromatogr. A 1058 (2004) 209.
[10] W. Weckwerth, Ann. Rev. Plant Biol. 54 (2003) 669.
[11] P. Kiefer, E. Heinzle, O. Zelder, C. Wittmann, Appl. Environ. Microbiol. 70 (2004) 229.
[12] J.C. Lindon, E. Holmes, J.K. Nicholson, Prog. Nucl. Magn. Reson. Spectrosc. 39 (2001) 1.
[13] O. Fiehn, J. Kopka, P. Dörmann, T. Altmann, R.N. Trethewey, L. Willmitzer, Nat. Biotechnol. 18 (2000) 1157.
[14] U. Roessner, L. Willmitzer, A.R. Fernie, Plant Cell Rep. 21 (2002) 189.
[15] W. Weckwerth, K. Wenzel, O. Fiehn, Proteomics 4 (2004) 78.
[16] P. Schoenmakers, P. Marriott, J. Beens, LC-GC Eur. 16 (2003) 335.
[17] R.E. Murphy, M.R. Schure, J.P. Foley, Anal. Chem. 70 (1998) 1585.
[18] R.C.Y. Ong, P.J. Marriott, J. Chromatogr. Sci. 40 (2002) 276.
[21] W. Weckwerth, M.E. Loureiro, K. Wenzel, O. Fiehn, Proc. Natl. Acad. Sci. U.S.A. 101 (2004) 7809.
[22] A.E. Sinha, B.J. Prazen, R.E. Synovec, Anal. Bioanal. Chem. 378 (2004) 1948.
[23] T. Adam, T. Ferge, S. Mitschke, T. Streibel, R.R. Baker, R. Zimmermann, Anal. Bioanal. Chem. 381 (2005) 487.